Demonstration of artificial visual percepts generated through thalamic microstimulation

John S. Pezaris* and R. Clay Reid

Department of Neurobiology, Harvard Medical School, 220 Longwood Avenue, Boston, MA 02115

Electrical stimulation of the visual system might serve as the foundation for a prosthetic device for the blind. We examined whether microstimulation of the dorsal lateral geniculate nucleus of the thalamus can generate localized visual percepts in alert monkeys. To assess electrically generated percepts, an eye-movement task was used with targets presented on a computer screen (optically) or through microstimulation of the lateral geniculate nucleus (electrically). Saccades (fast, direct eye movements) made to electrical targets were comparable to saccades made to optical targets. Gaze locations for electrical targets were well predicted by measured visual response maps of cells at the electrode tips. With two electrodes, two distinct targets could be independently created. A sequential saccade task verified that electrical targets were processed not in motor coordinates, but in visual spatial coordinates. Microstimulation produced predictable visual percepts, showing that this technique may be useful for a visual prosthesis.

primate | prosthesis | tetrode

The motivation to create a visual prosthesis is to restore sight to those who have become blind because of trauma of the eye or diseases such as glaucoma, macular degeneration, and retinitis pigmentosa. In these cases, the eye has ceased functioning as a sensory organ, but the remainder of the visual system is largely intact. By bypassing the eye and introducing appropriately processed externally generated signals into the visual path, the hope is that an analogue of vision can be created.

Research efforts in visual prostheses can be split into two broad approaches: those in which healthy retinal neurons are stimulated (1, 2), and those in which visual cortical neurons are stimulated (3–5). Retinal approaches have enjoyed some success, but have been hampered in part because of retinal fragility, which complicates implantation, and retinal architecture, which complicates electrical stimulation. Epiretinal devices, in which stimulating electrodes are placed on the vitreous surface of the retina adjacent to retinal ganglion cell bodies and axons (6), are currently being tested in human volunteers. Subretinal devices, in which stimulating elements are placed in the space behind the photoreceptors, are also being pursued, although one of the most advanced projects (7) is attempting to assist low-vision patients rather than restore sight to blind individuals.

Although cortical approaches have a long history of human experimentation (6, 8), the bulk of recent development has been in the cat and monkey (reviewed in ref. 9). One limitation of the cortical approach is that the representation of visual information becomes quite complex in the primary visual cortex (V1), such that evoked percepts may be quite different depending on the precise location of the stimulating electrodes. Cortical implants have also been limited by the large extent and vascularity of V1. Finally, the foveal portion of V1 in humans, representing the central part of visual space, is sometimes found buried in the interhemispheric fissure (10, 11), complicating the implantation of stimulating devices.

Our approach is to place stimulating electrodes in the dorsal lateral geniculate nucleus (LGN), the part of the thalamus that relays signals from the retina to V1. The LGN holds promise as a target of electrical stimulation for four reasons. First, the receptive fields (RFs) of LGN neurons are simple, well characterized (12), and similar to those in the retina. Stimulation of a small number of LGN neurons should achieve simple, focal percepts. Second, it has a macroscopic segregation of functional streams, in particular, the magnocellular and parvocellular pathways. Third, a single small craniotomy would provide access to neurons whose responses lie throughout the entire visual field. Unlike the retina, the fovea and parafovea are overrepresented spatially in the LGN, so that a dense sampling of neurons with central visual fields is possible. Unlike V1 in humans, the foveal representation is equally accessible as the periphery. Fourth, and perhaps most importantly, surgical access to the LGN would require relatively minor modifications to implant techniques currently used in human patients, because the LGN is physically adjacent to areas targeted for deep brain stimulation, a form of therapy for movement disorders such as Parkinson's disease (13, 14). Building on techniques already brought to clinical acceptability would ease the task of developing an LGN-based device.

We wanted to establish the feasibility of artificially creating visual percepts through electrical stimulation in the LGN. Our experiments were performed in alert monkeys so that we could use a behavioral report to assess the effects of stimulation. To determine what a monkey sees when electrical stimulation is applied to the LGN, we took advantage of the natural primate reaction to look at any suddenly illuminated point of light. This response was used to train monkeys to perform quick, direct eye movements, known as saccades, from one visual target to another. Our findings support the idea that electrical microstimulation in the LGN creates visual percepts, or phosphenes, that are interpreted as normal visual events.

Results

On a daily basis, we placed a microwire bundle electrode, or tetrode (15), in the LGN and mapped the visual responses (RFs) of cells for a given location of the electrode (16). We then used a center-out saccade task where the animal was required to sit in front of a computer screen and was rewarded for making saccadic eye movements from a central fixation point of light to a target point a short distance away. Trials with optical targets were interleaved with less frequent electrical-stimulation trials (and unstimulated trials, or blanks) to see whether the animal would treat electrical percepts in the same manner as the screen

PRE–FIXATION · **PAUSE** · **OPTICAL TARGET** · **SACCADE**

A1 · A2 · A3 · A4

ELECTRICAL

B1 · B2 · B3 · B4 ?

BLANK

C1 · C2 · C3 · C4 ?

0–1000 ms · 300 ms · 50–200 ms · 300 ms

measured eye position ⊙
fixation point ·
illuminated optical target ○
unilluminated target position ⋯
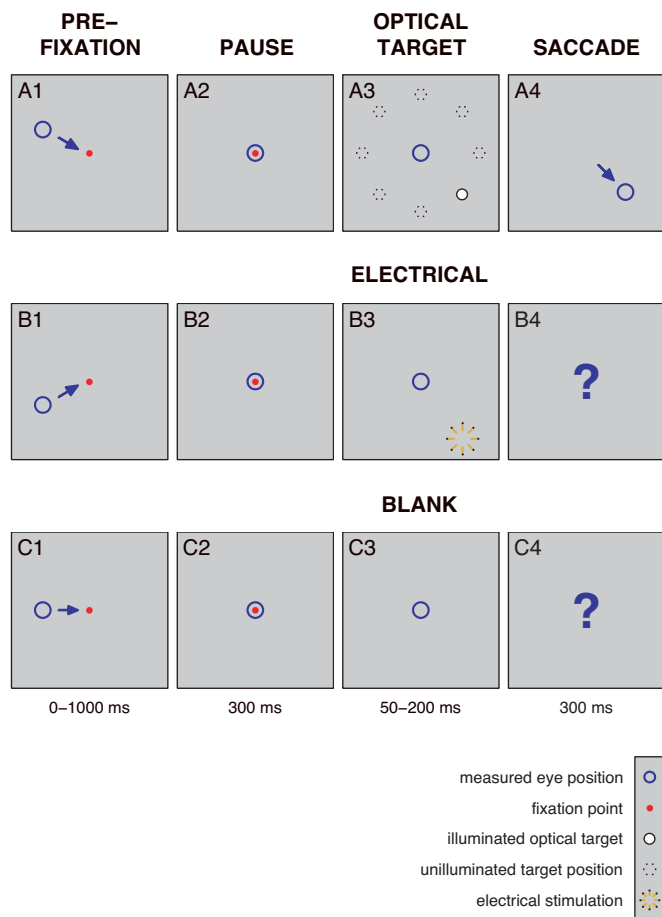electrical stimulation ☼

Fig. 1. The main behavioral task is shown. Each row represents one of the three conditions, optical (*Top*), electrical (*Middle*), and blank (*Bottom*). Optical trials were rewarded upon successful completion of the task; electrical and blank trials were rewarded on a random schedule with the same average rate as the optical percent correct. (*A1–A4*) Optical task: primary control. When presented with a fixation point (red dot) on a 50% gray background, the animal was required to shift gaze position (blue circle) so as to foveate it. After a brief delay, a target point (filled white circle) was flashed in one of eight possible locations and the animal was required to saccade to the target location; unused targets (dashed circles) are indicated in the diagram, but did not appear on the screen. (*B1–B4*) Electrical task: experimental manipulation. As in *A*, but the target was generated through electrical stimulation (yellow star). (*C1–C4*) Blank task: secondary control. As in *A*, but no target was presented.

Fig. 2. Example result showing electrical targets are like optical targets. Results are from a block of trials in the three conditions: optical (*A*), electrical (*B*), and blank (*C*) (see Fig. 1). Eye positions (black traces) for the saccade period, corresponding to Fig. 1 *A4*, *B4*, and *C4*, start at the center of each panel. Multiple trials are overlaid. (*A*) Optical condition. Saccade endpoints (dark blue circles) cluster around target positions (light blue cross-hairs). Offsets between saccade endpoints and target positions are typical of this task and were seen in both animals. (*B*) Electrical condition. Saccade endpoints (red circles) cluster at a position distinct from any of the optical targets. (*C*) Blank condition. Final gaze positions (green circles), measured at the end of the 300-ms saccade period, cluster near the origin, indicating no eye motions were elicited before the time window ends.

optical and electrical cases (see below). Because rewards on electrical and blank trials were given randomly at the same rate as correct optical trials (typically >95%), it would not have been possible for the animal to learn the RF location for electrical trials or any specific behavior for blank trials (see *Discussion*).

For some experiments, we examined the effects of varying stimulation amplitude to determine the threshold necessary to elicit saccadic responses (data not shown). Electrical stimulation was applied in both voltage controlled and current controlled mode (see *Materials and Methods* for pulse train specifics). The mean threshold to elicit a saccade response for current mode was $40 \pm 12 \mu A$ ($n = 6$, mean $\pm$ SD). The mean threshold for voltage mode was 2.5 ± 0.6 V ($n = 20$). The mean prestimulation electrode impedance was 540 ± 170 kΩ at 1 kHz ($n = 56$). Our equipment did not allow simultaneous monitoring of current and voltage. Current mode stimulation had significantly larger mean saccade endpoint cluster size ($1.2 \pm 0.6°$, $n = 14$) than voltage mode stimulation ($0.7 \pm 0.4°$, $n = 42$; $P < 0.01$, t test).

To compare endpoints in electrical trials against the visual responses for the electrode site, we overlaid the RF map (Fig. 3*A*) with the saccades elicited for electrical targets (Fig. 3*B*). There was a strong correspondence between the RF center and saccade endpoints, with saccade endpoints often covering the RF center. Sometimes a small offset was found between the RF center and saccade endpoints, but it was also found for optical targets (see *Discussion*), as is typical for tasks where saccadic targets are extinguished before eye movements commence (17). Similar results were found for locations spanning all four quadrants of the visual field at eccentricities of 2–26° (Fig. 3; quantitative detail below).

Saccadic reaction times were comparable between optical and electrical stimulation (animal a_1: 160 ± 18 ms vs. 172 ± 45 ms, mean $\pm$ SD, $n = 34$, $P > 0.1$, t test; animal a_2: 137 ± 10 ms vs. 127 ± 27 ms, $n = 22$, $P > 0.1$; Fig. 4 *A1* and *A2*). Because signals were being introduced into the LGN directly, bypassing the transduction delay at the retina, we might have expected 10- to 15-ms shorter latencies to electrical versus optical targets, but that was not consistently seen. For pooled data, the modes for electrical and optical latencies were 125 and 140 ms, respectively (5-ms bins), but this difference was not significantly reflected in

targets (Fig. 1). A block of 100–200 trials was presented in balanced pseudorandom order with respect to optical target position, electrical stimulation, and blank targets (10 conditions in all), for a given experiment. A total of 56 such experiments, each with different electrode placement, were performed in three LGNs of two adult monkeys.

Once animals performed consistently above 80% correct while training on optical targets alone, recordings commenced with all three types of trials (optical, electrical, and blank), and both animals were observed to immediately generalize to electrical targets in the task (see *Discussion*), treating electrical targets no differently from optical targets (Fig. 2). In the electrical condition, despite there being no cue on the computer screen, both animals made consistent saccades to a location corresponding to the measured visual response of that experiment's stimulation site (Figs. 2 and 3). In the blank condition, no saccade was observed in the allowed period for 25% of the trials, as in Fig. 2*C*; for the rest, saccades lacked tight clustering like
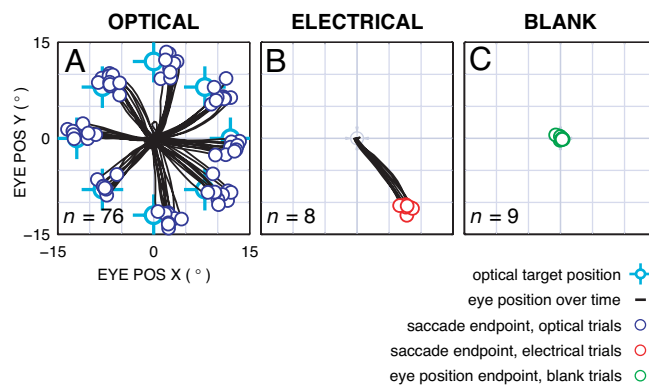
NEUROSCIENCE

Fig. 3. Comparison of RF center and electrical target saccade endpoints. (*A*) Example RF map. Measured from the same recording location as data for Fig. 2*B*, in register with the fixation point at the center of the panel. Red pixels correspond to locations where cells responded to white squares in the mapping stimulus (none in this example), blue pixels for responses to black squares, and gray pixels where there was no response. The area mapped is the extent of gray pixels (15 by 15 degrees, here). The response for this site is a one-pixel blue peak down and to the right of the fovea. (*B*) Overlaid RF map and electrical saccades. RF peak is highlighted (orange cross-hair). Overplotted saccades from Fig. 2*B* demonstrate correspondence between endpoints and RF location with an error comparable to that for optical targets (Figs. 2*A* and 4*B*). (*C–F*) Additional examples of correspondence between RF map and saccades in response to electrical targets. Similar results were found in all three LGNs studied, spanning all four quadrants of visual space, at eccentricities of 2–26°. (*G*) Summary of RF positions (blue dots) and saccade cluster centers (red diamonds). Errors for electrical saccades were comparable to, although somewhat larger than, those for optical saccades (Fig. 4*B*).

Fig. 4. Latency, accuracy, and repeatability. (*A1*, *B1*, and *C1*) Measures used to analyze saccade performance: latency (*A1*), error (*B1*), and scatter (*C1*). (*A2*, *B2*, and *C2*) Summary results from all three LGNs for optical and electrical saccades. Summary results are presented for the 56 experiments as box plots for optical (blue, *Left*) and electrical (red, *Right*) conditions depicting the 5th-, 25th-, 50th-, 75th-, and 95th-percentile levels in the lower bar, lower box edge, heavy bar, upper box edge, and upper bar, respectively. (*A1*) Latency was calculated as the difference in time between fixation offset (coincident with target onset) and saccadic response. The horizontal axis is time in a given trial. The two upper traces are the horizontal (magenta) and vertical (cyan) components of eye position. The two lower traces are the final portion of the fixation point (green box, enabled; green line, extinguished) and the period where the target was present (orange box and line) for either kind of target. (*A2*) Optical and electrical saccades had identical average latencies for pooled data, although the distribution of electrical saccades was wider (124/137/150/160/186 ms optical at 5/25/50/75/95 percentiles, 94/126/150/177/235 ms electrical). No significant differences were found between optical and electrical latencies for either animal. (*B1*) Error was calculated as the distance between target position or RF center and mean saccade endpoint. (*B2*) Optical error was slightly, but significantly, smaller than electrical error for pooled data (1.1/1.3/1.5/2.0/2.5° optical, 0.7/1.4/2.1/3.0/4.7° electrical, *P* < 0.0005). Individual animal data were similar. (*C1*) Scatter was calculated as the mean of the sizes of a 2D Gaussian fitted to the saccade endpoint positions (one-sigma contour shown). (*C2*) Optical and electrical scatter were very similar (0.4/0.5/0.7/1.0/1.3° optical, 0.2/0.4/0.6/1.1/1.7° electrical) without statistical significance for pooled data and for animal *a₁*, although for *a₂*, electrical scatter was significantly less than optical (*P* < 0.002). Underlined numbers indicate middle values.

the distance between the center of each cluster of saccade endpoints and the appropriate target: the screen location for optical stimuli, the RF location for electrical stimuli. For repeatability, we examined the size of endpoint clusters through the mean of major and minor axes of fitted 2D Gaussians.

The distance between saccade cluster center and appropriate target was somewhat greater for electrical (2.3 ± 1.2°, mean ± SD) than for optical (1.7 ± 0.5°) saccades, but the means were not significantly different for two of the three LGNs (*t* test: *P* > 0.3, *n* = 10, and *P* > 0.05, *n* = 22 for animal *a₁*/L, and *a₂*/R, but *P* < 0.005, *n* = 24 for *a₁*/R; Fig. 4 *B1* and *B2*). The additional error in the electrical condition was not large (difference in medians 0.3°, *n* = 56) and may be caused in part by the 1° resolution used when measuring RF position. Monte Carlo simulations show that quantization noise in RF position measurement contributes 0.1° to the mean observed error for electrical targets, explaining part, but not all, of the difference [see *Materials and Methods* and supporting information (SI) *Text*].

Repeatability, the size of endpoint clusters, was indistinguishable between optical and electrical saccades (0.8 ± 0.6° vs. 0.8 ± 0.5°, mean ± SD; Fig. 4 *C1* and *C2*) for pooled data, although animal 2 had significantly smaller scatter for electrical saccades

the means (155 ± 50 ms and 150 ± 39 ms, *P* > 0.07). Because the task did not require that the animals react as quickly as possible, the fairly large spread in latencies might have obscured slight differences. The speed-versus-distance relationship for saccades was indistinguishable between electrical and optical cases (*P* > 0.2, Kolmogorov-Smirnov test on the ratio; data not shown).

We examined saccade accuracy and repeatability to assess whether electrically evoked percepts were at the RF location of nearby LGN neurons, as expected. For accuracy we examined
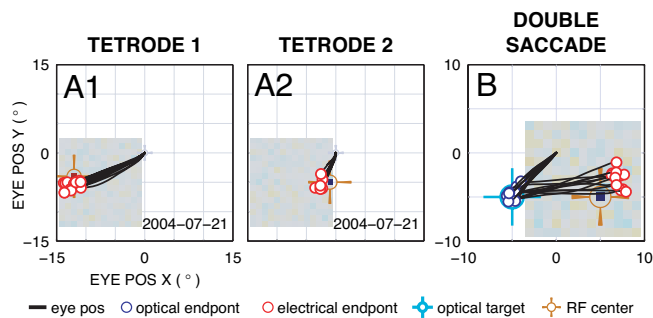
Fig. 5. Discrimination between two electrodes (*A1* and *A2*) and a two target task (*B*). (*A1* and *A2*) Single experiment performed with two concurrently implanted electrodes [Tetrode 1 (*A1*) and Tetrode 2 (*A2*)] slightly staggered along an oblique penetration in the LGN. The RF centers were separated in visual space by 10°. A variant of the primary experiment was performed where one electrode was randomly selected for stimulation in interleaved fashion for electrical trials. The animal discerned which electrode was stimulated 100% of the time. (*B*) A different experiment where two stimuli were presented in sequence, first, an optical stimulus to the lower left of fixation, and second, an electrical stimulus with an RF center to the lower right. Eye position traces start at the central fixation point, show a saccade to the lower left with accurate landing at the optical target position (light blue cross-hair), followed by a saccade to the right with accurate landing at the RF position (orange cross-hair) relative to the fixation point rather than to the optical target location or some intermediate point. This set of correct two-saccade sequences demonstrates that electrical stimulation is not directly evoking a saccade, but instead is creating a normal visual percept. The overshoot and upward shift to the second target was seen with two optical targets.

$(0.8 \pm 0.5°$ vs. $0.5 \pm 0.3°$, *t* test, $P < 0.01$). In contrast, the scatter of blank saccades, when they were present, was eight times worse at $6.5 \pm 3.4°$ (mean $\pm$ SD, pooled). Within the limits of our behavioral assay, the animals could thus localize electrically evoked percepts as accurately as the 0.5° optical targets and did not appear to localize any target during blank trials.

Electrical stimulation was performed in both parvocellular and magnocellular subdivisions of the LGN. Electrode tracks were inferred from a 3D model of LGN (18) by using a combination of electrode depth, alternation of eye input, and the RF location for each recording along a penetration to constrain site locations in the tissue. Thirty sites were tentatively identified as parvocellular and 26 as magnocellular with these criteria. No changes in statistical significance in the analysis presented above were found when selecting either magnocellular or parvocellular sites alone. Additionally, no significant differences were found for the electrical saccade latency (Kolmogorov–Smirnov tests: $P > 0.8$), accuracy ($P > 0.8$), or repeatability ($P > 0.2$) in magnocellular versus parvocellular sites, although this bears additional investigation with more definitive laminar identification.

A small number of experiments (two in each animal) were performed with two tetrodes to simultaneously access different RF locations. Electrodes were placed 10–15° apart in visual space, and both animals were able to distinguish between interleaved stimulation to the two with 100% accuracy (Fig. 5 *A1* and *A2*). The discrimination threshold for spatial separation between two points was not tested.

The results presented thus far do not rule out the possibility that electrical stimulation in our task directly drives saccades, for instance, by engaging motor pathways via retinal collaterals to the superior colliculus (19) or by retrograde stimulation of tectothalamic projections from the superior colliculus (20), rather than generating a visual percept to which the animal reacts. We therefore performed additional experiments (two in each animal) in which two targets were presented in quick succession and the animals were required to saccade to them sequentially. Both targets (50 ms long) in this protocol were

extinguished before the animals began to respond, although the temporal separation of the targets varied from block to block (30–80 ms). During training, both targets were optical; during subsequent data collection, the first target was optical and the second electrical. Both animals were able to perform the dual saccade task correctly (performance was >70% for optical target followed by optical target, and for optical target followed by electrical target conditions). If the electrical and optical targets interfered, or if the phosphene was not perceived in spatial coordinates, the second saccade might be expected to land at a location relative to the first target, or a point between the fixation point and the first target. Instead the second saccade was to the RF center as originally measured relative to the fixation point (Fig. 5*B*), suggesting the electrical target created a phosphene that was interpreted in spatial coordinates unaffected by the intervening optical saccade.

Discussion

The primate visual system includes three early stages of processing and therefore three candidate targets for visual prostheses: retina, LGN, and V1. As discussed below, perceptual results for single-electrode stimulation in the three areas are comparable. This finding suggests that other factors such as surgical accessibility, robustness of tissue, and biocompatibility may be more important for the development of a visual prosthesis.

Perceptual results from retinal stimulation in humans have been inconsistent. Humayun *et al.* (21) reported annular percepts 1.5° across with a coaxial electrode (central wire with encircling return) placed intraoperatively on the human retina. With other electrode shapes and configurations, they reported round percepts in addition to less symmetric ones, such as lines and rectangles, ≈0.5–1.5° in size. In one chronically implanted patient, they reported similar sizes for single-electrode stimulation (22). Rizzo *et al.* (23) intraoperatively placed a retinal array electrode in human volunteers and simulated through individual contacts or combinations of contacts. A variety of percepts were reported, many of which were not predictable from the stimulation configuration. Single-contact stimulation most commonly generated single percepts ≈0.5–5.0° across, although at times pairs or constellations of percepts were seen.

Although early attempts at cortical stimulation in humans used relatively large surface electrodes with high current levels (3, 6, 24), recent approaches achieved far better results with penetrating microelectrodes terminating in cell body layers. Schmidt *et al.* (25) working in human visual cortex stimulated between single microelectrodes and a remote return and reported pinpoints or disks of light (≈1° maximum). Percepts were described as points, some with color, where increasing superthreshold current generally produced smaller and whiter percepts. In some cases, single-electrode stimulation evoked multiple phosphenes. Tehovnik *et al.* (26) used electrical stimulation between single electrodes and remote return to interfere with an optical target presented near the RF of the stimulating electrode site in monkey V1. Results from that study suggest that evoked percepts were ≈0.6° in diameter for stimulation in the parafoveal area. Bradley *et al.* (27) performed a study similar to the present one, using indwelling microelectrodes in macaque V1 and assessing perceptual characteristics by using a memory-saccade task. On average they found saccades to electrical targets had larger scatter than those to optical targets (2.4° vs. 1.0°). The mean error (distance between RF and saccade endpoints) for electrical targets was ≈4°, but the mean optical error was not reported. Bradley *et al.*'s figures are slightly larger than the present results; the differences are likely caused, in part, by differences between their task and the one used in the present study, such as the length of time between stimulus and response.

Our efforts to develop an LGN approach have followed the established path of beginning with single electrodes and gener-

alizing to multiple electrodes. Summarizing our results, we found that LGN microstimulation evokes percepts that were treated as if they were presented visually. Without explicit reinforcement, animals responded to electrical stimuli with saccades that were similar or identical in latency, repeatability, and speed metrics from those evoked by optical stimuli (Fig. 4 and *Results*), and with a high degree of correspondence between phosphene locations and RF position (Figs. 3 and 4). Experiments with two electrodes and two targets (Fig. 5 *A1* and *A2*) demonstrated the expandability of this technique to more complex stimuli, although certainly substantial work remains to determine the interaction between simultaneously stimulated electrodes.

Care was taken to avoid cuing or mistraining the animals in these experiments. Each day's electrode placement was different and precise RF locations were not cued through any of the screen stimuli. Electrical trials appeared infrequently (1 in 10) and were rewarded on a random schedule based on ongoing optical performance, as any fixed schedule (including 0% or 100%) might have cued a difference in allowed behavior. For both animals, optical-only training preceded data collection for many weeks; both animals made accurate saccades to the RF position for the first block once electrical trials were enabled (animal a_1, error 2.3°, scatter 0.5°; a_2, 1.2°, 0.6°), demonstrating an immediate generalization for electrical targets in the task.

The dual-saccade task showed that electrical stimuli can be treated on the same footing as optical stimuli (Fig. 5*B*). If, for instance, electrical stimulation directly evoked saccades, we would expect only a single saccade in response, either directly to the electrical target or to a weighted average of the optical and electrical target positions. Instead, two normal saccades were seen, first to the optical target, and then to the electrical target, suggesting that the animal's visual system treated the electrical stimulus as a normal visual input and that the phosphene was perceived in spatial rather than retinotopic coordinates. That is, the planned endpoint did not shift despite an intervening gaze shift. Phosphenes in this condition have thus been successfully introduced into the visual stream, including processing by higher-order areas that abstract a stable perception of the external world despite continual eye movements. Microstimulation in the LGN created a visual, rather than incongruous, event.

Of the three main potential targets for prosthetic stimulation of the visual system, the LGN provides a number of advantages. First, existing clinical methods used for deep brain stimulation (13, 14) can be adapted for use in an LGN-based prosthesis by increasing the number of electrode contacts. As the human LGN is an oblate structure 6–7 mm on a side with a volume of 250 ± 50 mm³ (28), a sampling density even as coarse as 1 mm in three dimensions would therefore provide 200–300 phosphene points spanning visual space. This is thought to be enough for facial recognition and assisted reading (24, 29, 30), although a denser array would be expected to provide a higher grade of restored function. A simpler 2D array of electrodes, approximately coplanar to the curved extent of a single LGN lamina, could have 40–60 electrode tips in the LGN (data not shown). Although the development of an appropriate high channel-count stimulator would be required to drive such large collections of electrodes, this concern is true of any current visual prosthesis project. Second, regular spacing of electrodes in LGN will create a perceptual spacing highly weighted toward the central visual field. Retinal implants do not share this advantage; although V1 implants do, because of convolutions in the cortical surface, it is not a simple matter to cover the entire visual field. Finally, the LGN is an architecturally more attractive target for stimulation than the retina or V1. The center-surround RFs of the retina are preserved at the LGN, but the parvocellular, magnocellular, and koniocellular streams are segregated throughout the LGN unlike either the retina or V1.

In summary, the LGN is an attractive stimulation target for a visual prosthesis. It has the advantages of foveal magnification and comparatively simple representation and architecture. Our results suggest that the tremendous development effort required to create a clinical device may well prove fruitful. In particular, the widespread use of deep brain stimulation techniques provides good evidence that surgical accessibility is not a barrier. Further experiments with patterned stimulation through an array of electrodes should help demonstrate whether the LGN approach can create richer visual percepts, such as motion and shape, that would be necessary for a visual prosthesis.

Materials and Methods

Subjects. Two normal adult macaque monkeys (*Macaca mulatta*), one female and one male, were used in these experiments. The animals were chair-trained and familiarized with the laboratory and handler before experiments commenced. A structural MRI was taken to guide the implantation of a cylindrical titanium recording chamber over a chronically maintained craniotomy with a vertical approach to the identified location of the LGN (31). Additionally, a titanium head post was affixed to the skull with titanium bone screws, and a scleral search coil was implanted in one eye (32) with leads routed to an external connector at either the head post or the recording chamber. Surgical manipulations were performed by using sterile techniques. All protocols had Institutional Animal Care and Use Committee approval and met National Institutes of Health and U.S. Department of Agriculture requirements on the care and use of animals.

Electrodes. Tetrodes were constructed out of 13- and 15-μm polyimide-coated tungsten wire (California Fine Wire, Grover Beach, CA) using a custom-built twister. Tetrodes were advanced through the craniotomy and into the brain by using a tapered transdural guide tube that was 32 ga (220 μm OD) for the distal 10 mm. For experiments with two tetrodes, both electrodes were advanced through the same guide tube, but were differentially trimmed so that the ends were staggered by 1.5–2.0 mm. Electrode position in the horizontal plane was controlled with an *X-Y* stage (FHC Inc., Bowdoinham, ME) and depth was controlled with a hydraulic microdrive (David Kopf Instruments, Tujunga, CA).

Eye Position. The field coil driver and receiver circuitry was custom built. Eye positions were calibrated and corrected to within 2% full-scale error spanning the central 25° of the computer monitor. Calibrations were found to be stable within a recording session, with only minor adjustments necessary from day to day (data not shown).

Apparatus. Training and recording sessions took place in a shielded, darkened room. Animals were seated in primate chairs (Crist Instrument Co., Hagerstown, MD) and placed 30 cm away from a computer monitor (model P225f; ViewSonic Corp., Walnut, CA) running at 800 by 600 pixels with 180-Hz vertical refresh. Individual pixels on the screen spanned ≈0.1° of visual space. Stimulus isolators (model 2200; A-M Systems, Sequim, WA) were driven in either voltage mode or current mode from a data sequencing and acquisition system (Power 1401; Cambridge Electronic Design, Cambridge, U.K.). Stimulation was 80- to 200-ms long trains of 1-ms sinusoidal pulses repeating at 100 or 200 Hz (42/56 were 200 Hz) for 10–40 pulses (27/56, a plurality, were 20 pulses). Stimulation was applied between neighboring leads of a single tetrode to ensure electric fields and currents would be highly focused and to limit the volume of activated tissue. Because stimulation was applied between neighboring wires in a bundle rather than a single electrode and a remote return, the initial polarity of the stimulus (cathodic or

anodic) was not uniquely defined. Behavioral control and stimulus presentation were performed with custom software. Offline analysis was performed in Matlab (Mathworks, Natick, MA).

Recording Location. A full-field alternating flicker stimulus was used to detect the LGN as electrodes were advanced ventrally. Electrodes were determined to be in the LGN when all of the following criteria were met: responses to the search task were robust and clearly lateralized with at least one contralateral to ipsilateral transition (or the reverse) during penetration; perisaccadic bursts of activity were observed with every eye movement; and an RF map could be obtained with peak location consistent with other penetrations. In one animal, MRI-visible depositions were used to verify the location of the LGN (33).

Track Reconstruction. Using the laminar identification based on a full-field alternating flicker stimulus and RF positions measured for each recording location in a single penetration, probable electrode tracks were computationally reconstructed by selecting volumes of tissue with matching characteristics in a model LGN (18). Combining this with the electrode X-Y position within the recording chamber and the interlocation distance along a penetration produced a likely penetration path and therefore laminar identification for each recording site.

RF Mapping. RF maps were measured through a fixation task separate from the primary experimental task. Once the animal had fixated, a white-noise stimulus consisting of a 15-by-15 checkerboard of 1° across, 100% contrast, black or white squares was shown over the RF location while neural activity was monitored. Sequence snippets 1–5 s long were used for each trial with 300- to 500-ms fixation before and after each snippet. Multiunit activity was reverse-correlated against the stimulus, pixel location by pixel location, to develop a response map according to standard techniques (19). Sequences were pseudo-random with repeat period larger than the total presentation used in an entire block of mapping trials.

Monte Carlo Simulation of RF Quantization Noise. Because RF centers were computed with 1° resolution, larger than the expected RF sizes for LGN at the 2–26° eccentricities studied (30), we performed a simulation to estimate the extent to which this uncertainty affected our electrical target error measurements. Data for optical targets, where the target location was set with 0.1° resolution, were used for this simulation. Optical target locations were perturbed in simulation with ±0.5° uniformly distributed noise in both x and y directions, equivalent to the quantization error for RF center measurements, and the incremental errors were determined for saccades to those targets as compared with unperturbed targets. One hundred simulations were performed with the entire set of optical targets, and the mean additional error was computed.

1. Rizzo JF, Wyatt J (1997) *Neuroscientist* 3:251–262.
2. Liu W, McGucken E, Vichienchom K, Clements SM, Demarco SC, Humayun M, de Juan E, Weiland J, Greenberg R, (1999) *Proc IEEE Int Conf Systems Man Cybernet* 4:364–369.
3. Dobelle WH, Mladejovsky MG, Girvin JP (1974) *Science* 183:440–444.
4. Normann RA, Maynard EM, Rousche PJ, Warren DJ (1999) *Vision Res* 39:2577–2587.
5. Troyk P, Bak M, Berg J, Bradley D, Cogan S, Erickson R, Kufta C, McCreery D, Schmidt E, Towle V (2003) *Artif Organs* 27:1005–1015.
6. Maynard EM (2001) *Annu Rev Biomed Eng* 3:145–168.
7. Chow AY, Chow VY, Packo KH, Pollack JS, Peyman GA, Schuchard R (2004) *Arch Ophthalmol* 122:460–469.
8. Margalit E, Maia M, Weiland JD, Greenberg RJ, Fujii GY, Torres G, Piyathaisere DV, O'Hearn TM, Liu W, Lazzi G, et al. (2002) *Surv Ophthalmol* 47:335–356.
9. Warren DJ, Normann RA (2005) *Vision Res* 45:551–565.
10. Dougherty RF, Kich VM, Brewer AA, Fischer B, Modersitzki J, Wandell BA (2003) *J Vision* 3:586–598.
11. Tootell RB, Hadjikhani NK, Vanduffel W, Liu AK, Mendola JD, Sereno MI, Dale AM (1998) *Proc Natl Acad Sci USA* 95:811–817.
12. Wiesel TN, Hubel DH (1966) *J Neurophysiol* 29:1115–1156.
13. Kumar R, Lozano AM, Kim YJ, Hutchison WD, Sime E, Halket E, Lang AE (1998) *Neurology* 51:850–855.
14. Limousin P, Krack P, Pollak P, Benazzouz A, Ardouin C, Hoffmann D, Benabid A-L (1998) *N Engl J Med* 339:1105–1111.
15. Wilson MA, McNaughton BL (1993) *Science* 261:1055–1058.
16. Reid RC, Victor JD, Shapley RM (1997) *Vis Neurosci* 14:1015–1027.
17. Hikosaka O, Wurtz RH (1983) *J Neurophysiol* 49:1268.
18. Erwin E, Baker FH, Busen WF, Malpeli JG (1999) *J Comp Neurol* 407:92–102.
19. Beckstead RM, Frankfurter A (1983) *Exp Brain Res* 52:261–268.
20. Harting JK, Huerta MF, Hashikawa T, van Lieshout DP (1991) *J Comp Neurol* 304:275–306.
21. Humayun MS, de Juan E, Dagnelie G, Greenberg RJ, Propst RH, Phillips DH (1996) *Arch Ophthalmol* 114:40–46.
22. Humayun MS, Weiland JD, Fujii GY, Greenberg R, Williamson R, Little J, Mech B, Cimmarusti V, Van Boemel G, Dagnelie G, de Juan E (2003) *Vision Res* 43:2573–2581.
23. Rizzo JF, Wyatt J, Lowenstein J, Kelly S, Shire D (2003) *Invest Ophthalmol Visual Sci* 44:5361–5369.
24. Brindley GS, Lewin WS (1968) *J Physiol* (*London*) 196:479–493.
25. Schmidt EM, Bak MJ, Hambrecht FT, Kufta CV, O'Rourke DK, Vallabhanath P (1996) *Brain* 119:507–522.
26. Tehovnik EJ, Slucum WM, Schiller PH (2004) *Eur J Neurosci* 20:264–272.
27. Bradley DC, Troyk PR, Berg JA, Bak M, Cogan S, Erickson R, Kufta C, Mascaro M, McCreery D, Schmidt EM, et al. (2005) *J Neurophysiol* 93:1659–1670.
28. Andrews TJ, Halpern SD, Purves D (1997) *J Neurosci* 17:2859–2868.
29. Cha K, Horch KW, Normann RA (1992) *J Opt Soc Am A* 9:673–677.
30. Zrenner E (2002) *Science* 295:1022–1025.
31. Scherberger H, Fineman I, Musallam S, Dubowitz DJ, Bernheim KA, Pesaran B, Corneil BD, Gilliken B, Andersen RA (2003) *J Neurosci Methods* 130:1–8.
32. Judge SJ, Richmond BJ, Chu FC (1980) *Vision Res* 20:535–538.
33. Fung SH, Burstein D, Born RT (1998) *J Neurosci Methods* 80:215–224.

NEUROSCIENCE